

A microbiologically clean strategy for access to the Whillans Ice Stream subglacial environment

JOHN C. PRISCU¹, AMANDA M. ACHBERGER², JOEL E. CAHOON³, BRENT C. CHRISTNER², ROBERT L. EDWARDS¹, WARREN L. JONES³, ALEXANDER B. MICHAUD¹, MATTHEW R. SIEGFRIED⁴, MARK L. SKIDMORE⁵, ROBERT H. SPIGEL⁶, GREGG W. SWITZER¹, SLAWEK TULACZYK⁷ and TRISTA J. VICK-MAJORS¹

¹Department of Land Resources and Environmental Science, Montana State University, Bozeman, MT 59717, USA

²Department of Biological Sciences, Louisiana State University, Baton Rouge, LA 70803, USA

³Department of Civil Engineering, Montana State University, Bozeman, MT 59717, USA

⁴Scripps Institution of Oceanography, University of California, San Diego, La Jolla, CA 92093, USA

⁵Department of Earth Science, Montana State University, Bozeman, MT 59717, USA

⁶National Institute of Water and Atmospheric Research Ltd, Box 8602, Christchurch, New Zealand

⁷Department of Earth and Planetary Sciences, University of California, Santa Cruz, Santa Cruz, CA 95064, USA

jpriscu@montana.edu

Abstract: The Whillans Ice Stream Subglacial Access Research Drilling (WISSARD) project will test the overarching hypothesis that an active hydrological system exists beneath a West Antarctic ice stream that exerts a major control on ice dynamics, and the metabolic and phylogenetic diversity of the microbial community in subglacial water and sediment. WISSARD will explore Subglacial Lake Whillans (SLW, unofficial name) and its outflow toward the grounding line where it is thought to enter the Ross Ice Shelf seawater cavity. Introducing microbial contamination to the subglacial environment during drilling operations could compromise environmental stewardship and the science objectives of the project, consequently we developed a set of tools and procedures to directly address these issues. WISSARD hot water drilling efforts will include a custom water treatment system designed to remove micron and sub-micron sized particles (biotic and abiotic), irradiate the drilling water with germicidal ultraviolet (UV) radiation, and pasteurize the water to reduce the viability of persisting microbial contamination. Our clean access protocols also include methods to reduce microbial contamination on the surfaces of cables/hoses and down-borehole equipment using germicidal UV exposure and chemical disinfection. This paper presents experimental data showing that our protocols will meet expectations established by international agreement between participating Antarctic nations.

Received 20 August 2012, accepted 25 November 2012, first published online 28 March 2013

Key words: clean access, environmental stewardship, hot water drilling, subglacial aquatic environments

Introduction

Recent discoveries of life under the thick ice sheet covering Antarctica have radically changed our view of the interior of the Antarctic continent. Subglacial exploration presents considerable challenges to the way we conduct science in an atmosphere of increasingly stringent environmental concerns (Priscu 2002, Priscu *et al.* 2003). Priscu *et al.* (1999) and Karl *et al.* (1999) were the first to show that there was microbial life in water from Subglacial Lake Vostok that had accreted to the bottom of the ice sheet. Since these seminal reports, others have confirmed the presence of microbial life both within and beneath Antarctica's ice sheet (e.g. Christner *et al.* 2006, Priscu *et al.* 2007, Lanoil *et al.* 2009). As such, the basal zones of ice sheets are now thought to harbour active microbial ecosystems and our view of the extent of Earth's biosphere has expanded substantially (Priscu & Christner 2004, Priscu *et al.* 2008).

The pristine nature of Antarctic subglacial ecosystems has led to international concern about environmental and scientific stewardship during their exploration. Following more than ten years of deliberation by international and national committees (e.g. NRC 2007, Priscu *et al.* 2010), it has become clear that sampling of lakes and sediments beneath Antarctica's ice sheets must be done in such a way that minimizes microbial and chemical contamination to the environment and to the samples being retrieved. All those involved in this research must recognize that environmental stewardship should take precedence over scientific endeavours. We can expect subglacial lakes to be at the forefront of the Antarctic tradition of melding interdisciplinary and international science in exploring one of the last unexplored frontiers on our planet (Priscu 2002).

Largely through the efforts of scientific specialists organized by SCAR, three major subglacial drilling projects are now underway (Priscu *et al.* 2005). These include the

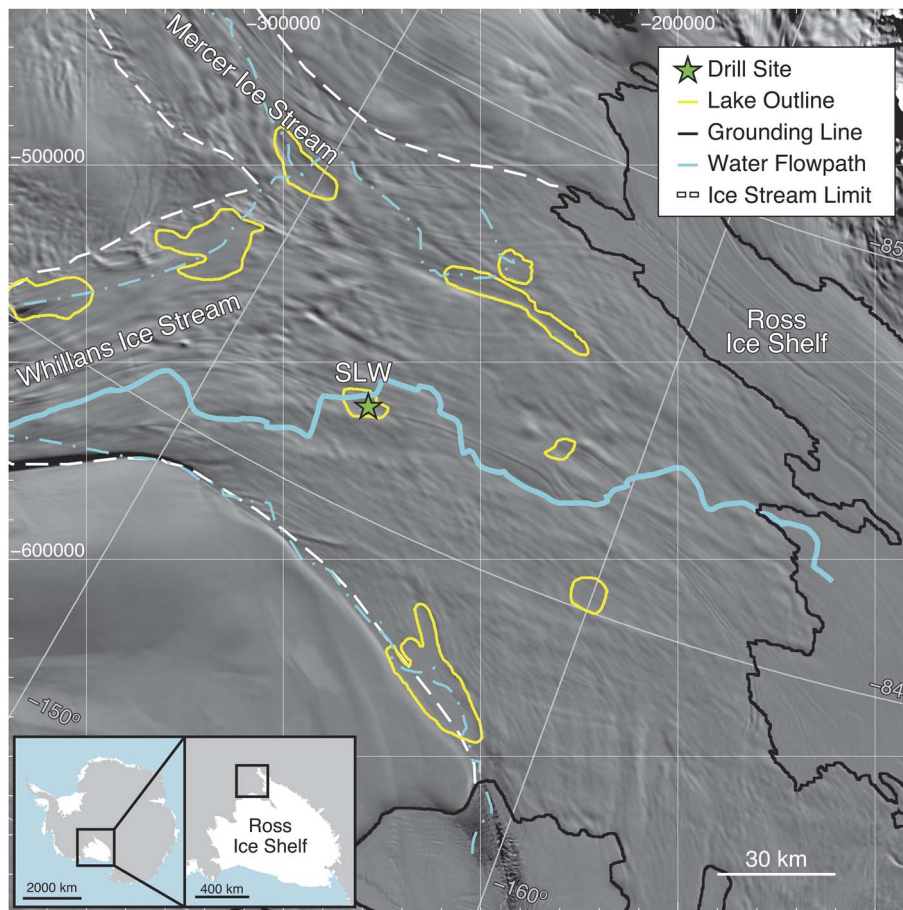


Fig. 1. Map showing the location of Subglacial Lake Whillans (green star = SLW, 84.237°S, 153.614°W) and its predicted flow path to the Ross Ice Shelf (heavy blue line). WISSARD sampling sites include the lake itself and near the end of the flow path close to the grounding line (heavy black line). The outlines of other lakes on the Whillans Ice Stream (yellow outlines) and their predicted flow paths (light blue lines) are also presented. Polar stereographic projection with true scale at -71°S; gridlines are spaced at 50 km intervals. Background imagery and grounding line are from the MODIS Mosaic of Antarctica (Scambos *et al.* 2007); lake outlines from MODIS image differencing (Fricker & Scambos 2009); ice stream boundaries were determined from InSAR velocities (Rignot *et al.* 2011); hypothesized water flow paths were determined by tracing continuous local hypopotential minima (Carter *et al.* 2011, Carter & Fricker 2012).

Lake Vostok programme funded by the Russian Antarctic Federation (Lukin & Bulat 2011), the Lake Ellsworth programme funded by the United Kingdom's Natural Environment Research Council (Ross *et al.* 2011), and the Whillans Ice Stream Subglacial Access Research Drilling (WISSARD) project, funded by the United States National Science Foundation (Fricker *et al.* 2011). All of these projects plan to access their subglacial targets within the next few years. Each project has proposed a suite of methods to ensure clean access to their respective systems, the details of which can be found on the Antarctic Treaty System's website as informational papers or comprehensive environmental evaluations (http://www.ats.aq/e/ats_keydocs.htm).

The WISSARD project proposes to sample subglacial lake Whillans (SLW) during the 2012–13 summer field season and the subglacial environment on the lower Whillans Ice Stream in a region near the grounding zone (GZ) during the 2013–14 summer season. The GZ site will be in an area where drainage from SLW is thought to enter the marine environment beneath the Ross Ice Shelf (Fig. 1). Access to the subglacial environment will be accomplished using a hot water drilling system to penetrate the ~800 m of ice overlying the basal water. To ensure that the borehole water

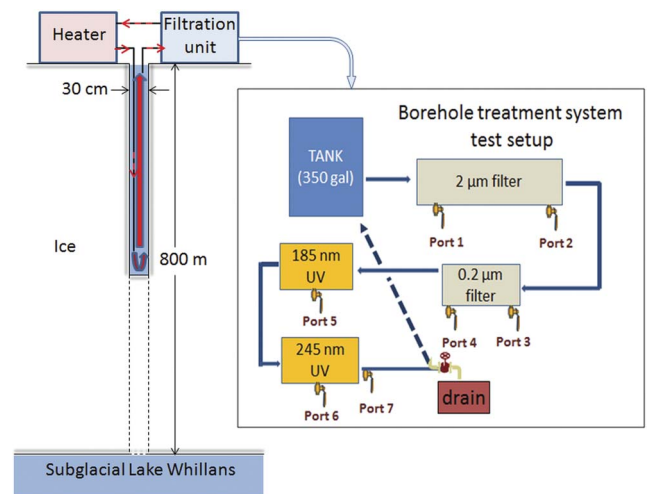


Fig. 2. Schematic (left panel, not to scale) showing the flow directions for the field operation of the Whillans Ice Stream Subglacial Access Research Drilling (WISSARD) water treatment system. The filtration and UV-treatment unit will be placed in-line between the borehole water return line and the heater modules. The enlarged inset (right panel) shows the treatment system components as set up for the laboratory tests. See text for details.

meets the cleanliness requirements promoted by a recent US National Research Council report (NRC 2007) and the scientific integrity of samples (water and sediments) is maintained, the project will include a borehole water treatment system designed to eliminate particles $> 0.2 \mu\text{m}$ in diameter, and reduce the concentration of viable microbial cells present in the borehole water (Fig. 2) and attached to deployed equipment and instrumentation.

This document presents: i) results from experiments designed to test the efficacy of the filtration system, and ii) disinfection protocols to be employed at all proposed WISSARD drilling sites where biological clean access is a requirement. These results are discussed within the context of the hydrology of SLW.

Methods

Borehole filtration and germicidal treatment system

The filtration component of the water treatment system consists of a $2 \mu\text{m}$ prefilter (pleated polypropylene cartridges, 15 cm diameter x 203 cm long, Champion Process Inc) followed by $0.2 \mu\text{m}$ filtration through a polyethersulfone membrane cartridge (7 cm diameter x 76 cm long, Champion Process Inc). After filtration, the clarified water was subsequently exposed in sequence to two separate ultraviolet (UV) irradiation modules (Glasco UV) that use 185 nm ozone-producing lamps followed by exposure to 254 nm germicidal lamps (wavelengths denote peak spectral output). Based on data supplied by the manufacturer, the tandem filtration strategy is designed to decrease the number of particles $> 0.2 \mu\text{m}$ by 99.98% (i.e. 4-log reduction). The two UV systems provide a 185 nm dosage $> 40\,000 \mu\text{W}\cdot\text{sec cm}^{-2}$ and 254 nm germicidal dosage $> 175\,000 \mu\text{W}\cdot\text{sec cm}^{-2}$. Doses of $40\,000 \mu\text{W}\cdot\text{sec cm}^{-2}$ are typically used for water disinfection, and depending on the UV transmission properties of the water and the sensitivity of the microorganisms to UV, exposures in this range have been shown to reduce the number of viable cells by 1-log to nearly 6-log (Aquafine Corp). The internal volume of the entire system (filters plus UV units) is 572 l. In a field scenario, the treated water will undergo a final pasteurization step where water temperature will progressively reach 90°C before exiting the 152 m long heating coils of the drilling unit. In summary, the WISSARD borehole water treatment system will use three complementary technologies to reduce microbial contaminants in the borehole water: i) filtration to remove particles $> 0.2 \mu\text{m}$, ii) UV irradiation (185 and 254 nm), and iii) pasteurization in the boilers of the hot water drill.

In field operations, hot water is pumped to the bottom of a 30 cm diameter borehole at high pressure (the diameter will be controlled by adjusting the water heating rate), flows upward in the hole and is pumped from the top, as shown schematically in the left-hand panel of Fig. 2. After water is pumped from the top of the borehole, it flows

into a 14 000 l holding tank, then through the filtration system followed by the heater modules before again being pumped to the drilling nozzle at the bottom of the borehole. The drilling speed is expected to be 1 m min^{-1} through most of the ice and the filtration system will be run continuously during drilling operations. The liquid water in the hole-drill-treatment system thus forms a recirculating system, with a liquid volume that increases as drilling proceeds. A 1900 l insulated melt tank will provide start-up water for the field system by melting snow using heated glycol pumped through a series of heat-radiating immersion plates that form a recirculation system. The components of the treatment system are illustrated in the right-hand panel of Fig. 2 as set up for laboratory testing.

The following laboratory tests were conducted to determine the efficacy of the system:

- 1) Dye study to determine the system flow characteristics.
- 2) Fluorescent micro-bead ($1\text{--}5 \mu\text{m}$) and microbial cell removal.
- 3) Silt ($1.2\text{--}63 \mu\text{m}$ particle size) removal.
- 4) Effect of UV exposure on viability of a model bacterium (*Escherichia coli* strain K-12).
- 5) Lakewater test to examine the filtration efficiency and disinfecting properties of the UV lamps on populations of natural aquatic microorganisms.
- 6) Lakewater pasteurization test to assess the influence of the heat generated by the hot water drill on microbial viability.

Dye test

A dye test was performed to examine the hydraulic residence-time characteristics of water in the treatment system. The system was filled with water containing fluorescent Rhodamine WT (water tracing) dye at a concentration of $\sim 9 \mu\text{g l}^{-1}$, and then flushed with dye-free tap water at 95 l min^{-1} for 25 min. The flow rate of 95 l min^{-1} is within the range of flow to be used during actual drilling operations. At this rate, the treatment system has a mean residence time (volume 572 l divided by a flow rate of 95 l min^{-1}) of 6 min. The test duration of 25 min therefore corresponds to 4.2 residence times. During the course of the test, discrete samples were collected to examine the dilution of the dye at port 7. Data from port 7 represents the integrated flow characteristics of the entire system (filter plus UV lamp canisters). All fluorescence measurements were made on a calibrated Turner Model 112 fluorometer fitted with a C5-60 excitation filter, a C56 emission filter, and F4T-4 lamp.

Bead removal experiment

Fluorescent beads (manufacturer nominal size range: $1\text{--}5 \mu\text{m}$, mean = $2.2 \mu\text{m}$) were added to the feed tank

containing 1325 l of tap water to a final concentration of $\sim 2 \times 10^5$ beads ml^{-1} and mixed thoroughly. The bead mixture in the feed tank was then pumped through the filtration and UV canisters (the UV lamps were off for this test) at $\sim 941 \text{ min}^{-1}$ until 1113 l had passed through the system (~ 12 min). The filtered water was sent to the drain (i.e. it was not recirculated through the system). Samples were then collected in clean quadruplicate vials from the source tank and from ports 1, 2, and 4 along the flow path (Fig. 2). The samples were vortexed vigorously for ~ 30 s and prepared for microscopic enumeration by filtering 10 ml of sample onto a black polycarbonate $0.2 \mu\text{m}$ filter. A Nikon 80i microscope with a Nikon B2-A filter cube was used to enumerate all samples. Percent efficacy of bead removal from each port was calculated as:

$$\left(\frac{\text{Geometric mean bead count in the tank} - \text{Geometric mean bead count at a selected port}}{\text{Geometric mean bead count in the tank}} \right) \times 100,$$

where the geometric mean = the Nth root of the product of N replicates.

Silt removal experiment

Local mineral soil was mixed with ~ 13 l of tap water and sieved through $63 \mu\text{m}$ mesh to form a silt/clay slurry. The slurry was added to 440 l of water in the holding tank to a final concentration of 0.395 g l^{-1} and pumped through the $2 \mu\text{m}$ filtration unit at 951 min^{-1} . The $0.2 \mu\text{m}$ filter and the UV systems were bypassed in this test. Outflow water from the filtration unit was returned to the holding tank yielding a recirculating system with constant volume. Samples were collected from the tank six times over a 40 min period, with a final sample collected 15 hours after the pump was turned on. Additional samples were collected at ports 1 and 2, four times over the 15 hour experiment. All samples were filtered onto Whatman GF/C filters (effective particle retention $1.2 \mu\text{m}$), dried for 24 hours at 100°C and weighed. Standard particle-size classifications (Vanoni 1975) typically specify a range of particle diameters of $4\text{--}62 \mu\text{m}$ for silt, and $0.24\text{--}4 \mu\text{m}$ for clay. The Stokes settling velocity for the largest silt particle ($62 \mu\text{m}$) is less than 0.2 cm s^{-1} , and is much smaller than the upward average flow velocity in the 30 cm diameter ice borehole of 2.2 cm s^{-1} corresponding to a flow of 951 min^{-1} . Silt entering the ice hole with meltwater during field operations would therefore be maintained in suspension and carried into the filtration unit.

Bacterial culture removal and viability test

Cultures of *Escherichia coli* strain K-12 were grown in 25% nutrient broth and added to the holding tank to a final concentration of $\sim 10^6$ cells ml^{-1} . After mixing with 1330 l of water in the holding tank for 30 min, triplicate samples

were collected from the tank to estimate the bulk bacterial concentration in the test water before it passed through the UV treatment system. The pump was turned on and 227 l was allowed to pass through the UV system in three single pass experiments at flow rates of 191 min^{-1} , 761 min^{-1} , and 1521 min^{-1} , with triplicate samples collected from port 7 (post UV treatment) in autoclaved 20 ml vials. Flushing the system with 227 l before sampling provided adequate time for the UV lamps to reach full output capacity, and allowed water in the UV system to be replaced five times before samples were taken. This ensured that all of the standing water in the UV canisters (total canister volume = 45 l) was replaced with amended tank water before sampling began. Colony forming units (CFU) from the initial inoculum and each sample were enumerated by standard dilution spread plating on nutrient agar followed by overnight incubation at 37°C , and again after two weeks of incubation. The two week incubation allowed assessment of the potential for the bacteria to recover from UV irradiation. The limit of quantification for this method is 300 CFU ml^{-1} for aqueous samples.

Lakewater bacterial removal and viability

Experiments were conducted on lakewater from the Montana State University campus. Lakewater (760 l) was sieved through a $125 \mu\text{m}$ mesh net to remove large debris and brought to 950 l with tap water in the holding tank. The cell count in the original pond water was 1.90×10^6 cells ml^{-1} and 1.52×10^6 cells ml^{-1} following dilution in the tank. The UV lamps were switched on for 5 min (allowing them to reach full capacity) before recirculating the water through all filters and both UV lamps at 761 min^{-1} . Four replicate 10 ml samples were collected from the tank over a period of 90 min at selected times following pump start-up for bacterial counts and determination of intracellular adenosine triphosphate (ATP) concentration. Bacterial samples were collected in 10 ml sterile glass vials, fixed with formalin (5% v/v final concentration), stained using the deoxyribonucleic acid (DNA) dye SYBR GoldTM, and enumerated by epifluorescence microscopy (Lisle & Priscu 2004). Cellular ATP concentration, a proxy for microbial biomass and viability (Karl 1980), was determined by concentrating cells in a 10 ml water sample on a $0.2 \mu\text{m}$ acrodisk syringe filter (Pall Corp). Adenosine triphosphate was extracted with the Microbial ATP Kit HS (BioThema Inc), and luminosity was measured with a Glomax 20/20 luminometer. The limit of detection for this method was 10^{-15} mol ATP ml^{-1} based on two standard deviations above the y-intercept in the ATP standard curve.

Lakewater pasteurization test

Water collected from a lake on the Louisiana State University campus containing an original cell density of 2.5×10^5 (estimated by SYBR- GoldTM epifluorescence

microscopic counts) was serially diluted with filtered lakewater to create two identical sets of cell concentrations ranging from 2.5×10^4 to 25 total cells ml^{-1} . A set of control dilutions was incubated at $\sim 25^\circ\text{C}$ while the other was heated to 85°C for 2 min to mimic the effect of pasteurization in the boilers of the hot water drill. Following exposure to heat, cell viability was assayed by measuring the respiratory reduction of the tetrazolium dye 2, 3-bis-(2-methoxy-4-nitro-5-sulphenyl)-(2H)-tetrazolium-5-carboxanilide (XTT) to formazan (Roslev & King 1993). This tetrazolium salt is reduced by active respiratory electron transport, forming a water soluble formazan dye measureable as absorbance at 490 nm and serves as a proxy for cell viability.

Surface-based cleaning experiments

Triplicate flat stainless steel ($2.5 \text{ cm} \times 10 \text{ cm}$) and transparent thermoplastic Poly(methyl methacrylate) (PMMA) ($5 \text{ cm} \times 10 \text{ cm}$) coupons, representative of materials comprising the down-borehole instrumentation, were contaminated with either *E. coli* K-12 or the endospore-former *Bacillus subtilis*. The coupons were then analysed for cell viability following treatment with 3% hydrogen peroxide. Before inoculation with bacteria, all materials

were rinsed with sterile Type 1 ($18.2 \text{ M}\Omega \text{ cm}^{-1}$) water and autoclaved. The coupons were immersed in cell inocula (1×10^7 cell ml^{-1} *E. Coli*, 4×10^6 cell ml^{-1} *B. subtilis*) for 1 min and allowed to air dry for 5 min before being sprayed five times with 3% H_2O_2 (which completely wetted the surfaces) and allowed to react with the bacteria on the coupons for 1 min. Controls consisted of triplicate contaminated coupons not sprayed with H_2O_2 .

A 10 cm^2 area of all control and H_2O_2 -treated samples were swabbed in triplicate using sterile polyurethane swabs moistened with sterile phosphate-buffered saline (PBS). Swabs were immediately placed into 10 ml of sterile PBS where they were sonicated and vortexed to release cells into the buffer. The 10 ml PBS solution containing the cells was then serially diluted (five dilutions) into sterile PBS. One-hundred μL of each dilution was spread plated in triplicate onto nutrient agar. The cultures were incubated aerobically at 37°C and colonies were enumerated following 18 hours and 72 hours of incubation. The limits of detection for this method, accounting for the area swabbed and the ensuing dilution is 300 CFU cm^{-2} .

Results

Dye test results

A dye test was conducted for 25 min (4.1 times the mean residence time of the system) to examine the rate at which the dye decreased in the system following a clean water flush. This is the same method as that used to experimentally determine the residence time distribution for a reactor (Dankwerts 1953), except that the step-change in dye concentration here is negative. Nevertheless, the results yield the same information.

Changes in dye concentration from test 2 showed an exponential decrease of dye concentration over time (Fig. 3) and were fitted with Eq. (1):

$$C(t) = C_1 - (C_1 - C_0) * (1 - \exp(-kt)), \quad (1)$$

where $C(t)$ = concentration at a given time (t), C_1 = initial dye concentration at $t = 0$, $C_1 - C_0$ = the change in concentration between time $t = 0$ and $t = \text{infinity}$ (C_0 represents the final, tap-water concentration), and k = exponential decay factor, which denotes $1/\text{residence time}$ ($1/\text{TR}$).

The fit to the experimental points is excellent ($r^2 = 0.99$), and as shown in Fig. 3, is very similar to the theoretical dilution curve predicted for the flushing of a continuously stirred tank reactor (CSTR). This can be expressed in non-dimensional form, in terms of the fraction of fluid in the tank that remains to be replaced or flushed out at time t , by:

$$(C(t) - C_0)/(C_1 - C_0) = 1 - \exp(-t/\text{TR}) = 1 - \exp(-kt), \quad (2)$$

with parameters C_1 and C_0 equal to those of the fitted curve, but decay constant $k = 1/\text{TR} = 0.1661 \text{ min}^{-1}$. Here TR is the mean residence time (6.0 min), computed from

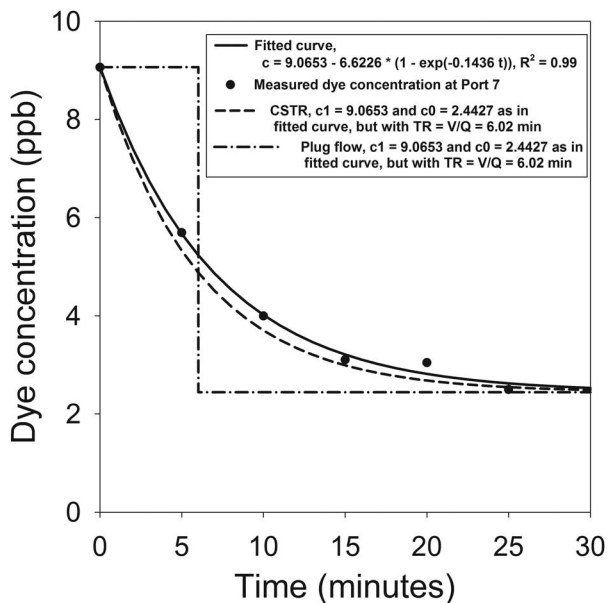


Fig. 3. Dye concentrations measured experimentally at Port 7 (filled circles); fitted exponential decay curve (solid line); the curve (dashed line) for a continuously stirred tank reactor (CSTR) with the same initial and final concentrations (C_1 and C_0) as for the fitted curve, but with the decay constant k computed from the mean residence time ($\text{TR} = V/Q$, $= 6.02$ min, where V = treatment system volume (5721) and Q = flow rate (951 min^{-1}), as $k = 1/\text{TR}$); and the curve (dashed-dot line) for a plug-flow reactor with the same initial and final concentrations (C_1 and C_0) as for the fitted curve, and residence time $\text{TR} = V/Q = 6.02$ min.

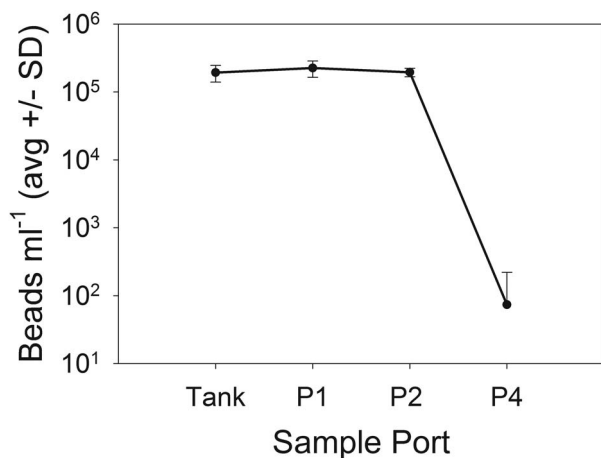


Fig. 4. Fluorescent beads counted from the tank and selected sample ports after filtering 11131 through the system. The flow rate was $\sim 941 \text{ min}^{-1}$. Error bars = standard deviation (SD) ($n = 4$).

the treatment system volume V and the experimental flow rate Q , as $TR = V/Q$ (Dankwerts 1953). Also shown in Fig. 3 is the theoretical flushing curve for plug-flow through the treatment system, which does not provide a good match to the treatment system's observed mixing and dilution behaviour. This is not surprising, given the complexity of internal flow paths through the various components of the treatment system.

The turnover or replacement fractions at various multiples of t/TR can be computed from Eq. (2), showing that one residence time ($t/TR = 1$) yields a turnover or replacement percent of 63%, and that it requires 3.0 and 4.6 residence times to replace 95% and 99%, respectively, of the fluid in the system. This equates to 95% and 99% replacement times for the fluid in the system of 21 min and 32 min, respectively for the flow of 951 min^{-1} .

Bead removal experiment

Bead concentrations at ports 1 and 2 were not significantly different ($P > 0.05$) from those in the tank after 11131 of water had passed through the $2 \mu\text{m}$ filter (Figs 2 & 4). However, bead concentration decreased by almost four orders of magnitude at port 4 after the sample water had passed the $0.2 \mu\text{m}$ filter ($P < 0.05$). The efficacy of bead removal by the $2 \mu\text{m}$ filter was essentially zero (there was no significant difference in bead concentration between the tank and samples at ports 1 and 2) while the $0.2 \mu\text{m}$ filter had a removal efficiency of $> 99\%$.

Silt removal experiment

The recirculation test using the $2 \mu\text{m}$ filter only showed that suspended sediment in the holding tank decreased

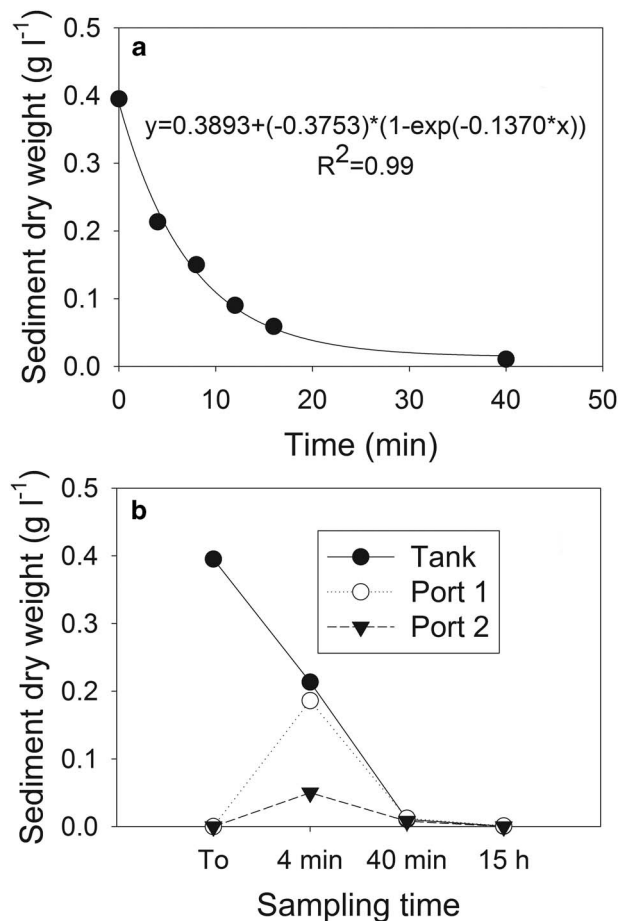


Fig. 5. a. Sediment concentration in the tank over time, and **b.** in the tank and ports 1 and 2 at specific times up to 15 hours. Water was recirculated through the tank during this experiment, passing only through the $2 \mu\text{m}$ filter, at a flow rate of 951 min^{-1} .

exponentially from 0.4 – 0.01 g l^{-1} over 40 min at a flow rate of 951 min^{-1} (Fig. 5a). The residence time of the system, calculated as $1/k$ from the fitted equation in Fig. 5a was 7.3 min. Both the shape of the removal curve and the value computed for the e-folding removal time closely match the flushing behaviour of the dye study. By analogy with the flushing described by Eq. (2), 95% and 99% of the sediment in the system would be removed in 22 and 34 min, respectively, under the experimental conditions.

Data from the inlet (port 1) and outlet (port 2) from the $2 \mu\text{m}$ filter system, showed that the dry weight of the sediment particles (63 – $1.2 \mu\text{m}$ in diameter) increased during the first 4 min interval after the pump was turned on, then dropped to background levels in the tank (Fig. 5b). These data indicate rapid mixing before filtration (port 1 data) and that a large number of particles were not retained in the initial pass through the filter. After 15 hours, no silt and clay particles were detectable (detection limit = 0.002 g l^{-1}) in samples from the tank,

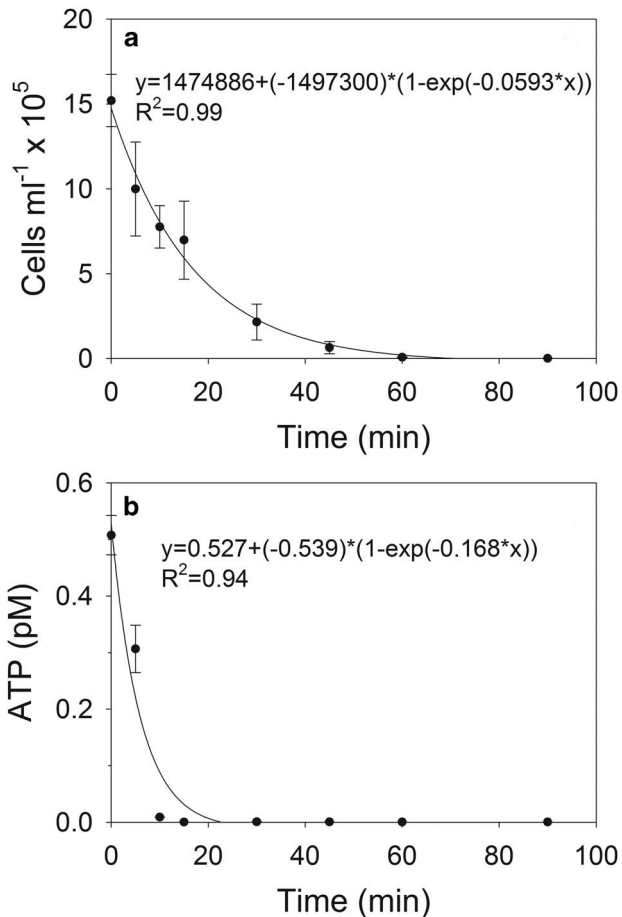


Fig. 6. a. Pond water cell, and **b.** adenosine triphosphate (ATP) concentrations in the tank at a flow rate of 761 min^{-1} with the samples passing through both filter systems and both UV lamps. Each time point represents the mean and standard error (s.e.) ($n = 3$). Cell concentrations and ATP levels were below levels of detection after 60 min and 15 min, respectively.

port 1, or port 2 (Fig. 5b). The final sampling time at 15 hours is 75 times the theoretical hydraulic retention time of the system.

UV exposure and cell viability

Circulation of the *E. coli* suspension through the 185 nm and 254 nm UV irradiation modules reduced the number of viable *E. coli* cells in the tank (initial concentration of $7.2 \times 10^6 \text{ CFU ml}^{-1}$) to below the methodological limit of quantification ($< 300 \text{ CFU ml}^{-1}$) on a single pass through the UV lamps at flow rates of 19, 76 and 1521 min^{-1} , which represents 2.7, 0.68 and 0.34 min of UV exposure as the sample passed through the UV system (based on a UV canister volume of 52l). After two weeks of incubation at room temperature ($\sim 22^\circ\text{C}$), the CFUs on the plates remained below 300 CFU ml^{-1} ,

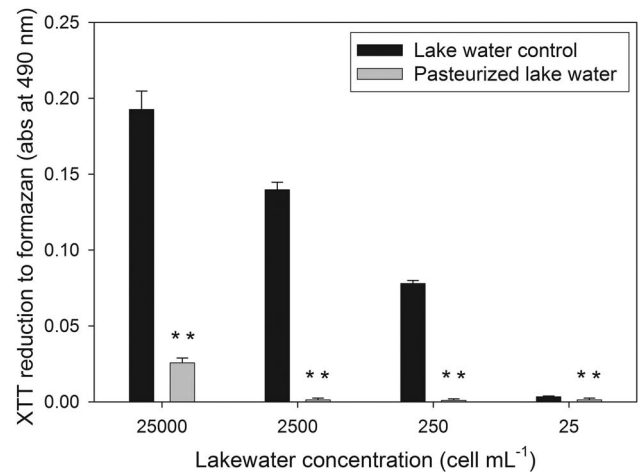


Fig. 7. Respiratory potential, detected as tetrazolium dye 2, 3-bis-(2-methoxy-4-nitro-5sulphenyl)-(2 H)-tetrazolium-5-carboxanilide (XTT) reduction to formazan dye (measured as absorption at 490 nm) of pasteurized (85°C for 2 min) lakewater samples relative to unpasteurized lakewater controls (no heat treatment) following 21 hours of incubation with XTT. The data represent a dilution series made from the original lakewater sample. Bars represent mean and 1 SD ($n = 3$). Asterisks denote that pasteurization significantly ($P < 0.001$) reduced cell viability in all dilutions.

providing evidence that the bacteria were killed by the UV treatment as opposed to incurring a level of sub-lethal damage that allowed them to remaining viable and recover.

Lakewater bacterial removal and viability

Viable lakewater bacteria within the tank were either physically removed or their DNA was irreversibly damaged by UV radiation during a 90 min experiment, reaching levels similar to that observed in procedural blanks by the end of the experiment (Fig. 6a). Based on the 761 min^{-1} flow rate used in this experiment and the exponential curve fit shown in Fig. 6a, 99% of all bacteria were removed or killed following 78 min of run time (51 min for 95% removal).

Adenosine triphosphate measurements from the tank over the course of the experiment revealed that cellular ATP decreased by three orders of magnitude (to the limits of detection of the ATP method) following 15 min of circulation (Fig. 6b). Based on the exponential model used to fit the data, 99% of ATP-containing cells were eliminated from the system (through a combination of cell removal by the filters and decomposition by the UV lamps) in 27 min (18 min for 95% removal) at the 761 min^{-1} flow rate used in the experiment. The almost three times greater reduction in ATP concentration relative to total cell number indicates that intracellular ATP was actually destroyed by the system, presumably by the UV lamps and

associated ozone. The reduced levels of intracellular ATP could also be the result of the synthesis of ATP-dependent enzymes used to repair UV damaged cells.

Lakewater pasteurization test

The pasteurization experiment (85°C for 2 min) conducted on lakewater showed that heating to the temperatures expected in the boiler of the hot water drill (at least 85°C) reduced respiration potential (XTT reduction to formazan dye) of the organisms significantly ($P < 0.001$) at cell densities ranging from 25–25 000 cell ml⁻¹ (Fig. 7). These results indicate that the boilers in the hot water drill can produce up to a 2-log reduction in the number of viable cells.

Surface cleaning experiments

Following experimental contamination with *E. coli* and *B. subtilis*, the stainless steel coupons averaged (\pm SD) $8.7 \times 10^4 \pm 8.6 \times 10^4$ CFU cm⁻² and $7.2 \times 10^4 \pm 4.0 \times 10^4$ CFU cm⁻², respectively. The averages (\pm SD) for these same organisms on the plastic coupons were $6.2 \times 10^5 \pm 1.8 \times 10^5$ CFU cm⁻² and $4.0 \times 10^5 \pm 3.9 \times 10^5$ CFU cm⁻², respectively. A one-way analysis of variance (ANOVA) followed by a multi-comparison test revealed that a significantly ($P < 0.001$) greater proportion of *E. coli* and *B. subtilis* adhered to the plastic coupons per unit area than the stainless steel coupons. No significant difference ($P > 0.05$) in adherence was evident between the test organisms. Following treatment with H₂O₂, plate counts after 18 hours and 72 hours of incubation were below the limits of quantification (300 CFU cm⁻²; i.e. no colonies formed), indicating a 2 to 3-log reduction in the concentration of viable cells.

Discussion

A flow rate of 95 l min⁻¹ and a total volume for the entire treatment system (filtration plus UV components) of 572 l yields a mean retention time of 6 min, which represents the time when 63% of the water in the system is replaced for a CSTR. Timescales for the system for 95% and 99% water replacement are 21 min and 32 min, respectively, at this flow rate. Results from the dye study yielded a dilution curve for the treatment system that was very similar to that for a CSTR. Moreover, the filtration-disinfection-heater-borehole forms a recirculating system, whereby water in the borehole continually recirculates through the treatment system as the borehole volume increases during drilling operations (i.e. the borehole is deepened). The expected drilling rate of ~ 1 m min⁻¹ (producing an increase in the water volume in a 0.3 m diameter borehole at a rate of 71 l min⁻¹) is slower than the upward velocity of water in the 30 cm diameter borehole (~ 1.3 m min⁻¹ at a flow rate of 95 l min⁻¹). Hence, water in the borehole is being

pumped through the filtration system at a faster rate than the liquid volume of the borehole is increasing.

The nature of mixing of water in the borehole itself is uncertain. Assuming an ice borehole depth and diameter of 800 m and 0.3 m, respectively (yielding a borehole volume of 57 m³), and a system pumping rate of 95 l min⁻¹, the mean residence time for borehole water would be ten hours. This would be the actual time for complete replacement of the water in the borehole if plug-flow results from water being pumped into the bottom of a relatively smooth borehole and removed from the surface at the same rate where it enters the filtration/UV system and boilers before being returned to the bottom of the borehole. Although flow in the actual borehole will be complicated by buoyancy effects (it is likely to be turbulent; Reynolds number ~ 4500), its mixing and replacement-time characteristics will resemble plug-flow much more closely than that of a CSTR (Dankwerts 1953). Hence, it is reasonable to assume that the timescale for complete replacement of borehole water will be of the same order as the mean residence time (ten hours), rather than that given for a CSTR (i.e. 4.6 times the mean residence time for 99% replacement).

As the heated water enters the bottom of the borehole, it will mix with newly melted water. The mixed water will start to flow upward in the borehole to maintain continuity with the rate at which water is being withdrawn at the surface for treatment and reheating. The question of how much, and how often, water in the borehole is treated is difficult to answer, because of this mixing, the complicated flow in the borehole, and the fact that the borehole volume grows with time. If the filtration system is run continuously during borehole drilling, as planned, the water volume in the borehole will be much less than 57 m³ during the early stages of drilling when the borehole depth is considerably shallower than 800 m, and borehole water originally near the surface will be passed through the water treatment system many times before the subglacial environment is entered. However, as the hole becomes very deep, a point will be reached beyond which there is not enough time for water melted at the bottom of the hole to reach the surface before the hole is melted to the base of the ice. Importantly, all of the heated water introduced into the bottom of the borehole will have passed through the treatment system at least once as the borehole reaches its maximum depth of ~ 800 m.

Based on our experimental results with sediment removal (Fig. 5b), one pass through the 2 μ m filter of the filtration system alone will not eliminate all of the sediment particles in the borehole, particularly if the sinking rate of sediment particles (> 63 μ m) exceeds the upward velocity of water through the borehole. However, the UV component of the system, which was shown to reduce *E. coli* by 4-log units following a single pass through the system at 95 l min⁻¹ and to reduce cellular ATP levels to below the limits of detection (10^{-15} mol ATP ml⁻¹)

following 15 min at 761min^{-1} , should significantly reduce the number of viable microbial cells. Hence, both systems working in tandem will effectively eliminate most of the relatively buoyant particles, including cells, in the system and kill a majority of the cells as melting proceeds from the surface to the bottom of the ice stream ($\sim 800\text{ m}$).

Our pasteurization tests showed that a lake microbial assemblage exposed to 85°C for 2 min significantly ($P < 0.001$) reduced the respiratory potential of the assemblage, resulting in up to a 2-log reduction in the number of viable cells. These conditions are similar to the temperatures and retentions of the boilers on the hot water drill. As such, the heating system alone on the WISSARD drill should kill the vast majority of bacteria that pass through it, particularly if they are not heat tolerant (e.g. not endospore-forming bacteria), which we expect to be the case for most of the bacteria that exist in the ice we will melt to generate the borehole water (e.g. Christner *et al.* 2008, Priscu *et al.* 2008).

In summary, our test results indicate that one passage of a volume of water through the filtration component of the system will reduce the total number of microbes by more than 4-log units. Any cells remaining in the water after filtration will be reduced another 3.5-log units by combined effect of UV irradiance and pasteurization. To place this into context, if we assume an initial borehole cell concentration of 10^6 cell ml^{-1} (equivalent to coastal ocean waters), the system as tested would be capable of reducing the microbial burden to $< 100\text{ cells ml}^{-1}$ in the borehole water after one borehole residence time (\sim ten hours at a 951min^{-1} pumping rate). Because we will treat all down borehole equipment with 3% H_2O_2 , which produced a 2 to 3-log reduction in our endospore and non-endospore forming test organisms, any cellular contamination introduced into the drilling and water treatment system during our operation is expected to be minimal. In addition to the safeguards discussed above, all hoses and cables on the WISSARD drilling system will pass through a clamp-on high pressure hot water cleaning system followed by a UV collar as they are deployed down the borehole. The UV collar will provide a disinfection dose of $40\,000\ \mu\text{W}\cdot\text{sec cm}^{-2}$ at a maximum cable/hose deployment rate of 60 m min^{-1} .

In addition to the filtration/UV system and decontamination protocols that will be implemented during borehole drilling, the hydraulic nature of the lake itself provides a safeguard against permanent contamination by drilling procedures. Subglacial Lake Whillans belongs to the category of active subglacial lakes, which are located and defined on the basis of anomalously fast ice surface changes attributed to large water volume fluctuations in subglacial lake basins. Active subglacial lakes were discovered by InSAR (Gray *et al.* 2005) and subsequent studies using satellite altimetry have demonstrated that there are > 120 such lakes in Antarctica (Wingham *et al.* 2006,

Fricker *et al.* 2007, Fricker & Scambos 2009, Smith *et al.* 2009). Active subglacial lakes are different from many previously described Antarctic subglacial lakes (e.g. review in Siegert *et al.* 2005) in a number of important ways. The defining feature of active subglacial lakes is that they actively fill and drain, undergoing volume changes large enough to cause localized, anomalously high (up to several metres) deformation of the ice surface above them that can be detected by a space borne instrument (e.g. Fricker *et al.* 2007). They also tend to occur within fast flowing parts of the Antarctic ice sheet (ice streams and outlet glaciers) as opposed to non-active lakes that are concentrated near ice divides, where ice flow is sluggish (Siegert *et al.* 2005, Smith *et al.* 2009). The active subglacial lakes discovered thus far tend to have a smaller area, and presumably volume, than their non-active counterparts. This may be largely due to observational biases because non-active lakes have been traditionally identified from airborne ice-penetrating radar surveys, which are more likely to encounter large subglacial lakes than small ones (e.g. Siegert *et al.* 2005). At the same time, active subglacial lakes have only been mapped using anomalous ice surface elevation changes occurring within the last decade, when new airborne/satellite altimetry and InSAR data provided sufficiently precise measurements of ice surface topography to reveal their existence. Hence, detection of such lakes is more likely if they have relatively small water residence time (i.e. high water throughput rates combined with low total basin volume).

Analyses of satellite data by Fricker *et al.* (2007) and Fricker & Scambos (2009) indicated that SLW has an area of $59\text{ km}^2 \pm 12\text{ km}^2$ and it has experienced two drain-fill cycles between 2003 and 2009. These authors estimated that each of the drain-fill cycles resulted in lake volume fluctuations of about 0.1 km^3 of water. The WISSARD surface geophysics team completed a high-density survey focused on the SLW basin in the 2010–11 field season. Improved constraints on ice geometry indicate that the subglacial water volume change during fill-drain cycles of SLW is 0.15 km^3 (unpublished data), which is 50% greater than the previous estimates of Fricker *et al.* (2007) and Fricker & Scamos (2009). Geophysical estimates of the depth of the lake at the time of the field survey, when the lake was drained, reveals that it is $< 8\text{ m}$ (Horgan *et al.* 2012, Christianson *et al.* 2012). The relatively shallow depth of the SLW basin is consistent with its location within a region of gently undulating basal topography and low ice surface slope (e.g. Shabtaie *et al.* 1987). Given the area of the lake basin, the lake volume can be estimated to be $< 0.5\text{ km}^3$. Consequently, it would take fewer than three to four fill-drain cycles to exchange the total lake volume. Given that SLW has undergone two complete fill-drain cycles over a six year period, we estimate a water residence time for the lake of the order of ten years, or less.

The decadal scale flushing time for SLW is nearly 100 times faster than that predicted for Subglacial Lake Ellsworth (SLE) (750 years; Siegert *et al.* 2012) and about 1000 times faster than the water residence time estimated for Subglacial Lake Vostok (~10 000 years; Bell *et al.* 2002). Clearly, SLW is fundamentally different from SLE and Vostok, which contain large water volumes and do not show evidence of significant water volume changes over the period of instrumental observations. Subglacial Lake Whillans can be considered a small temporary storage basin for water draining beneath the Whillans Ice Stream and any disturbance resulting from drilling and sampling operations should have a minor and transitory impact.

Acknowledgements

We are grateful to the Department of Civil Engineering for allowing us use of the Hydraulics Laboratory at MSU. P.W. Adkins assisted with the experiments and laboratory work and R. Powell commented on the manuscript. This work was supported by NSF-OPP grants 0838933 to JCP, 0838941 to BC and 0839142 to ST as part of the Whillans Ice Stream Subglacial Access Drilling (WISSARD) Project. We appreciate the support and contributions of the WISSARD science team, and drilling and operational support contractors in accomplishing our goals. We gratefully acknowledge the constructive comments of the reviewers.

References

- BELL, R.E., STUDINGER, M., TIKKU, A.A., CLARKE, G.K.C., GUTNER, M.M. & MEERTENS, C. 2002. Origin and fate of Lake Vostok water frozen to the base of the East Antarctic ice sheet. *Nature*, **416**, 307–310.
- CARTER, S.P. & FRICKER, H.A. 2012. The supply of subglacial meltwater to the grounding line of the Siple Coast, West Antarctica. *Annals of Glaciology*, **53**, 267–280.
- CARTER, S.P., FRICKER, H.A., BLANKENSHIP, D.D., YOUNG, D.A., JOHNSON, J.V., PRICE, S.F. & LIPSCOMB, V. 2011. Modeling five years of subglacial lake activity in the MacAyeal Ice Stream catchment through assimilation of ICESat laser altimetry. *Journal of Glaciology*, **57**, 1098–1112.
- CHRISTIANSON, K., JACOBEL, R.W., HORGAN, H.J., ANANDAKRISHNAN, S. & ALLEY, R.B. 2012. Subglacial lake Whillans: ice-penetrating radar and GPS observations of a shallow active reservoir beneath a West Antarctic ice stream. *Earth and Planetary Science Letters*, **331**, 237–245.
- CHRISTNER, B.C., SKIDMORE, M.L., PRISCU, J.C., TRANTER, M. & FOREMAN, C.M. 2008. Bacteria in subglacial environments. In MARGESIN, R., SCHINNER, F., MARX, J.-C. & GERDAY, C., eds. *Psychrophiles: from biodiversity to biotechnology*. New York: Springer, 51–71.
- CHRISTNER, B.C., ROYSTON-BISHOP, G., FOREMAN, C.M., ARNOLD, B.R., TRANTER, M., WELCH, K.A., LYONS, W.B., TSAPIN, A.I. & PRISCU, J.C. 2006. Limnological conditions in Subglacial Lake Vostok, Antarctica. *Limnology and Oceanography*, **51**, 2485–2501.
- DANKWERTS, P.V. 1953. Continuous flow systems. Distribution of residence times. *Chemical Engineering Science*, **2**, 1–13.
- FRICKER, H.A. & SCAMBOS, T. 2009. Connected subglacial lake activity on lower Mercer and Whillans ice streams, West Antarctica, 2003–2008. *Journal of Glaciology*, **55**, 303–315.
- FRICKER, H.A., SCAMBOS, T.A., BINDSCHADLER, R.A. & PADMAN, L. 2007. An active subglacial water system in West Antarctica mapped from space. *Science*, **315**, 1544–1548.
- FRICKER, H.A., POWELL, R., PRISCU, J.C., TULACZYK, S., ANANDAKRISHNAN, S., CHRISTNER, B., HOLLAND, D., HORGAN, H., MIKUCKI, J., MITCHELL, A., SCHERER, R. & SEVERINGHAUS, J. 2011. Siple Coast subglacial aquatic environments: the Whillans Ice Stream Subglacial Access Research Drilling (WISSARD) project. In SIEGERT, M.J., KENNICUTT II, M.C., BINDSCHADLER, R.A., eds. *Antarctic subglacial aquatic environments*. *American Geophysical Union Geophysical Monograph*, **192**, 199–219.
- GRAY, L., JOUGHIN, I., TULACZYK, S., SPIKES, V.B., BINDSCHADLER, R. & JEZEK, K. 2005. Evidence for subglacial water transport in the West Antarctic Ice Sheet through three-dimensional satellite radar interferometry. *Geophysical Research Letters*, **10.1029/2004GL021387**.
- HORGAN, H.J., ANANDAKRISHNAN, S., JACOBEL, R.W., CHRISTIANSON, K., ALLEY, R.B., HEESZEL, D.S., PICOTTI, S. & WALTER, J.I. 2012. Subglacial Lake Whillans: seismic observations of a shallow active reservoir beneath a West Antarctic ice stream. *Earth and Planetary Science Letters*, **331–332**, 201–209.
- KARL, D.M. 1980. Cellular nucleotide measurements and applications in microbial ecology. *Microbiological Reviews*, **44**, 739–796.
- KARL, D.M., BIRD, D.F., BJORKMAN, K., HOULIHAN, T., SHACKELFORD, R. & TUPAS, L. 1999. Microorganisms in the accreted ice of Lake Vostok, Antarctica. *Science*, **286**, 2144–2147.
- LANOIL, B., SKIDMORE, M., PRISCU, J.C., HAN, S., FOO, W., VOGEL, S.W., TULACZYK, S. & ENGELHARDT, H. 2009. Bacteria beneath the West Antarctic Ice Sheet. *Environmental Microbiology*, **11**, 609–615.
- LISLE, J.T. & PRISCU, J.C. 2004. The occurrence of lysogenic bacteria and microbial aggregates in the lakes of the McMurdo Dry Valleys, Antarctica. *Microbial Ecology*, **47**, 427–439.
- LUKIN, V. & BULAT, S. 2011. Vostok Subglacial Lake: details of Russian plans/activities for drilling and sampling. In SIEGERT, M.J., KENNICUTT II, M.C., BINDSCHADLER, R.A., eds. *Antarctic subglacial aquatic environments*. *American Geophysical Union Geophysical Monograph*, **192**, 187–197.
- NRC (NATIONAL RESEARCH COUNCIL). 2007. *Exploration of Antarctic subglacial aquatic environments: environmental and scientific stewardship*. Washington, DC: National Academies Press, 166 pp.
- PRISCU, J.C. 2002. Commentary: subglacial lakes have changed our view of Antarctica. *Antarctic Science*, **14**, 291.
- PRISCU, J.C. & CHRISTNER, B. 2004. Earth's icy biosphere. In BULL, A.T., ed. *Microbial diversity and prospecting*. Washington, DC: ASM Press, 130–145.
- PRISCU, J.C., POWELL, R.D. & TULACZYK, S. 2010. Probing subglacial environments under the Whillans Ice Stream. *EOS Transactions*, **91**, 253–254.
- PRISCU, J.C., CHRISTNER, B.C., FOREMAN, C.M. & ROYSTON-BISHOP, G. 2007. Biological material in ice cores. In ELIAS, S.A., ed. *Encyclopedia of Quaternary sciences*. Vol. 2. Amsterdam: Elsevier, 1156–1166.
- PRISCU, J.C., TULACZYK, S., STUDINGER, M., KENNICUTT II, M.C., CHRISTNER, B.C. & FOREMAN, C.M. 2008. Antarctic subglacial water: origin, evolution and ecology. In VINCENT, W. & LAYBOURN-PARRY, J., eds. *Polar lakes and rivers*. Oxford: Oxford University Press, 119–135.
- PRISCU, J.C., KENNICUTT II, M.C., BELL, R.E., BULAT, S.A., ELLIS-EVANS, C., LUKIN, V.V., PETIT, J.-R., POWELL, R.D., SIEGERT, M.J. & TABACCO, I. 2003. An international plan for Antarctic subglacial lake exploration. *Polar Geography*, **27**, 69–83.
- PRISCU, J.C., KENNICUTT II, M.C., BELL, R.E., BULAT, S.A., ELLIS-EVANS, C., LUKIN, V.V., PETIT, J.-R., POWELL, R.D., SIEGERT, M.J. & TABACCO, I. 2005. Exploring subglacial Antarctic lake environments. *EOS Transactions*, **86**, 193–200.
- PRISCU, J.C., ADAMS, E.E., LYONS, W.B., VOYTEK, M.A., MOGK, D.W., BROWN, R.L., MCKAY, C.P., TAKACS, C.D., WELCH, K.A., WOLF, C.F., KIRSSTEIN, J.D. & AVCI, R. 1999. Geomicrobiology of subglacial ice above Lake Vostok, Antarctica. *Science*, **286**, 2141–2144.
- RIGNOT, E., MOUGINOT, J. & SCHEUCHL, B. 2011. Ice flow of the Antarctic Ice Sheet. *Science*, **333**, 1427–1430.

- ROSLEV, P. & KING, G.M. 1993. Application of a tetrazolium salt with a water-soluble formazan as an indicator of viability in respiring bacteria. *Applied and Environmental Microbiology*, **59**, 2891–2896.
- ROSS, N., SIEGERT, M.J., RIVERA, A., BENTLEY, M., BLAKE, D., CAPPER, L., CLARKE, R., COCKELL, C., CORR, H., HARRIS, W., HILL, C., HINDMARSH, R., HODGSON, D., KING, E., LAMB, H., MAHER, B., MAKINSON, K., MOWLEM, M., PARNELL, J., PEARCE, D., PRISCU, J.C., SMITH, A., TAIT, A., TRANTER, M., WADHAM, J., WHALLEY, B. & WOODWARD, J. 2011. Subglacial Lake Ellsworth, West Antarctica: its history, recent field campaigns and plans for its exploration. In SIEGERT, M.J., KENNICUTT II, M.C., BINDSCHADLER, R.A., eds. *Antarctic subglacial aquatic environments*. *American Geophysical Union Geophysical Monograph*, **192**, 221–233.
- SCAMBOS, T., HARAN, T., FAHNESTOCK, M., PAINTER, T. & BOHLANDER, J. 2007. MODIS-based Mosaic of Antarctica (MOA) data sets: continent-wide surface morphology and snow grain size. *Remote Sensing of Environment*, **111**, 242–257.
- SHABTAIE, S., WHILLANS, I.M. & BENTLEY, C.R. 1987. The morphology of Ice Streams A, B, and C, West Antarctica, and their environs. *Journal of Geophysical Research*, **92**, 8865–8883.
- SIEGERT, M.J., CARTER, S., TABACCO, I., POPOV, S. & BLANKENSHIP, D.D. 2005. A revised inventory of Antarctic subglacial lakes. *Antarctic Science*, **17**, 453–460.
- SIEGERT, M.J., CLARKE, R.J., MOWLEM, M., ROSS, N., HILL, C.S., TAIT, A., HODGSON, D., PARNELL, J., TRANTER, M., PEARCE, D., BENTLEY, M.J., COCKELL, C., TSALOGLOU, M.N., SMITH, A., WOODWARD, J., BRITO, M.P. & WAUGH, E. 2012. Clean access, measurement, and sampling of Ellsworth Subglacial Lake: a method for exploring deep Antarctic subglacial lake environment. *Reviews in Geophysics*, 10.1029/2011RG000361.
- SMITH, B.E., FRICKER, H.A., JOUGHIN, I.R. & TULACZYK, S. 2009. An inventory of active subglacial lakes in Antarctica detected by ICESat (2003–2008). *Journal of Glaciology*, **55**, 573–595.
- VANONI, V.A. 1975. *Sedimentation engineering*. ASCE Manual 54. Prepared by ASCE Task Committee for the preparation of the manual on sedimentation of the Sedimentation Committee of the Hydraulics Division. Reston, VA: American Society for Civil Engineering, 418 pp.
- WINGHAM, D.J., SIEGERT, M.J., SHEPHERD, A. & MUIR, A.S. 2006. Rapid discharge connects Antarctic subglacial lakes. *Nature*, **440**, 1033–1036.